Available online at www.sciencedirect.com

ScienceDirect

IFAC PapersOnline CONFERENCE PAPER ARCHIVE

IFAC PapersOnLine 54-10 (2021) 7–14

Modelling and Output Predictive Control of Engine Air Path Systems for Intake Fresh-air and Exhaust Gas Recirculation

Yusuke Makimoto ** **Yuhki Hashimoto** *** **Yuto Kawamoto** **
Ikuro Mizumoto * **Hiromitsu Ohmori** ***

* *Faculty of Advanced Science and Technology, Kumamoto University, Kumamoto, Japan (e-mail: ikuro@gpo.kumamoto-u.ac.jp)*
** *Department of Mechanical System Eng., Kumamoto University, Kumamoto, Japan*
*** *Department of System Design Engineering, Keio University, Kanagawa, Japan (e-mail: ohmori@keio.jp)*

Abstract: This paper deals with the control problem of an engine air path system with low pressure exhaust gas recirculation (EGR). The considered air path system with low EGR can be modelled as a system with time-delays due to the transport delay of gas flow from EGR. It results in over intake fresh air, and thus it causes torque overshoot. An output predictive control system is designed for a time delay air path system in order to obtain the desired fresh air mass flow. In the considered system, the intake fresh air mass flow and the EGR rate are taken as the outputs, and the throttle valve and the EGR valve are considered as inputs of the system in this paper. A detailed air path system model with time-delay will also be derived for confirming the effectiveness of the proposed method through numerical simulations.

Keywords: air-path system modelling, air-path control, output predictive control, parallel feedforward compensator

1. INTRODUCTION

The combustion engine technologies have been highly developed during recent decade due to requirements of high combustion efficiency and low emission. The exhaust gas recirculation (EGR) is one of the effective ways to improve the combustion efficiency and to achieve low emission. Especially low pressure EGR is recently attracted a great deal of attention. By constructing low pressure EGR air path system, it is expected to reduce the nitrogen oxide (NOx) and intake loss without loss of turbine flow rate. However, since the low pressure EGR system has long path length, the transport delay of gas flow from EGR causes over and/or under intake fresh air in the intake manifold as illustrated in Fig. 1. This affects fuel consumption, and causes a torque overshoot and/or deterioration of the ride quality in the automobiles. To effectively control the air path system with the EGR is valuable to exploit the air path system's ability. As well known, most conventional control technique for engines have been based on the feedforward controls by look-up tables, so called 'control maps'. However, since engine systems have higher nonlinearities and might be sensitive to disturbances and the change of environment, developing the control maps for feedforward control requires a lot of time and effort with number of experiments to obtain in-depth data in order to make an accurate control map. Therefore, it is expected to develop robust control strategies with respect to changes of environment and disturbances for engine control in order to achieve high-performance of engine.

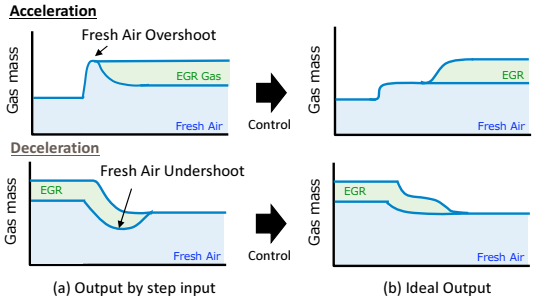

Fig. 1. Control objective

As one of the advanced control for engine, the model predictive controls (MPC) have been applied to engine control systems and have been researched actively in recent decade for controlling the air path system of engines (Herceg et al., 2006; Ferreau et al., 2007; Ortner et al., 2009; Gelso and Lindberg, 2014; Kekik and Akar, 2019). However, in order to apply the MPC for nonlinear systems having some constraints, nonlinear optimization problem and/or quadratic programing (QP) problem have to be solved online, and in the most cases, all the states of the system have to be available. This might be a strong restriction to apply the MPC method to engine air path control. Moreover, the application of the MPC is based on the applicability of the accurate model of the considered controlled system. With this in mind, an adaptive type feedforward control has also been proposed (Nielsen et al., 2017), and good control performance has been shown. However, the detailed structure of the nonlinearity of the

10.1016/j.ifacol.2021.10.133

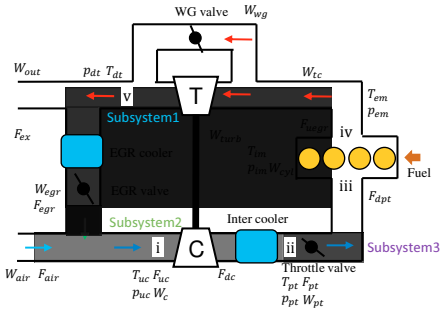

Fig. 2. Air Path System

system is required in order to derive an inversion of the input nonlinearity in the method.

Recently, an output prediction based robust predictive control strategy has been proposed (Mizumoto et al., 2015; Mizumoto and Fujii, 2017; Mizumoto et al., 2018). Unlike the conventional MPC methods, this method can design predictive control only using the measured output without all states of the system. However, the method did not handle the systems with a time delay.

In this paper, we consider applying the predictive control method in Mizumoto et al. (2018) to engine air path systems with EGR having a transfer delay of gas flow as a time delay of the system. The method in Mizumoto et al. (2018) is modified for systems with time delays by considering the existing time delay outside of the virtual augmented system with a parallel feedforward compensator(PFC) which renders an augmented system having relative degree of 1 and minimum-phase. Moreover, we derive an detailed mean value model of air path system based on the physical relations. The EGR transfer delay can be modelled as a time varying delay in the obtained model. The effectiveness of the proposed method is confirmed through numerical simulations via the obtained air path system model.

2. MODEL OF ENGINE AIR PATH SYSTEM

The considered engine air path system in this paper is illustrated as in Fig. 2. It is a 4-cylinder SI engine with a low pressure EGR. The variables and parameters in the engine model are defined as in Table. 1 and 2.

2.1 Model of Oxygen Concentration

We first derive an oxygen concentration model based on a physics-based time-varying transport delay (PTD) oxygen concentration modeling method (Zeng and Wang, 2014).

Let us consider subsystems 1 to 3 as in Fig. 2,and suppose that the gas is mixed instantly and the concentration is kept constant in each subsystem. A model of gas transportation and mixing in a control volume is illustrated in Fig. 3

The mixing model of gas in a control volume is given by

$$\dot{F}_{cv} = \frac{RT_{cv}}{p_{cv}V_{cv}} \sum_i [(F_{in,i} - F_{cv})W_{in,i}] \ , \tag{1}$$

Table 1. Physical Quantity

Symbol	Physical Quantity
p [Pa]	Pressure
T [K]	Temperature
F [%]	Oxygen Concentration
W [kg/s]	Mass flow rate
P [W]	Power
V [m^3]	Volume
A [m^2]	Area
L [m]	Subsystem length
r [m]	Subsystem radius
N_e [rpm]	Engine speed
u [%]	Valve opening
R [J$\cdot$kg$^{-1}\cdot$K^{-1}]	Gas constant
c_p [J$\cdot$kg$^{-1}\cdot$K^{-1}]	Specific heat at constant pressure
κ [-]	Heat capacity ratio
η_m [-]	Mechanical efficiency
η_t [-]	Turbine efficiency
η_c [-]	Compressor efficiency
τ [-]	Time constant of turbo charger
λ [-]	Cylinder efficiency

Table 2. Suffix

Suffix	Place of air pth system
air	Fresh air
uc	Up-Compressor
c	Compressor
dc	Down-Compressor
ic	Intercooler
pt	Pre-throttle
dpt	Down-pre-throttle
im	Intake-Manifold
cyl	Cylinder
em	Exhaust-Manifold
ex	Exhaust
wg	Waste-Gate
turb	Turbine
dt	Down-Turbine
out	Discharge to ambient
uegr	Up-Exhaust Gas Recirculation
egr	Exhaust Gas Recirculation
amb	Ambient

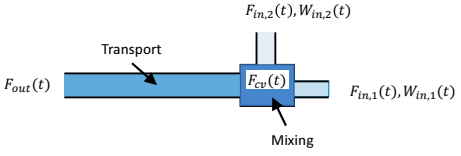

Fig. 3. Gas transportation and mixing model

where F_{cv} is the oxygen concentration in the control volume, $F_{in,i}$ is the oxygen concentration at i-th intake flow and $W_{in,i}$ is the mass flow rate at i-th intake flow.

Supposing that the gas velocity is obtained by

$$v = \frac{RT_{cv}\sum_i W_{in,i}}{p_{cv}\pi r^2} \ , \tag{2}$$

the transfer distance D of gas in a subsystem can be obtained as

$$D(t) = \int_{t_0}^{t} v(\tau)d\tau \tag{3}$$

Thus, if the transfer time in the subsystem is $\delta(t)$, then it leads

$$D(t_0 + \delta(t_0)) = L \tag{4}$$

For this transfer time $\delta(t)$, it follows that

Table 3. Correspondence of parameters for pressure and temperature

subsystem	F_{out}	$F_{in,1}, F_{in,2}$	$W_{in,1}, W_{in,2}$	F_{cv}	T_{cv}	p_{cv}	V_{cv}	r	L
subsystem1	F_{egr}	$F_{ex}, -$	$W_{egr}, -$	F_{uegr}	T_{dt}	p_{dt}	V_{dt}	r_1	L_1
subsystem2	F_{dc}	F_{egr}, F_{air}	W_{air}, W_{egr}	F_{uc}	T_{uc}	p_{uc}	V_{uc}	r_2	L_2
subsystem3	F_{dpt}	$F_{dc}, -$	$W_c, -$	F_{pt}	T_{pt}	p_{pt}	V_{pt}	r_3	L_3
Intake manifold	-	$F_{dpt}, -$	$W_{pt}, -$	F_{im}	T_{im}	p_{im}	V_{im}	-	-

r_j, L_j:Radius and length of subsystem j

Table 4. Correspondence of parameters for pressure and temperature

Place	p_O	V_O	$W_{O,1}, W_{O,2}$	T_O	$W_{I,1}, W_{I,2}$	$T_{I,1}, T_{I,2}$
i	p_{uc}	V_{uc}	$W_c, -$	T_{uc}	W_{air}, W_{egr}	T_{amb}, T_{egr}
ii	p_{pt}	V_{pt}	$W_{pt}, -$	T_{pt}	$W_c, -$	$T_{ic}, -$
iii	p_{im}	V_{im}	$W_{cyl}, -$	T_{im}	$W_{pt}, -$	$T_{pt}, -$
iv	p_{em}	V_{em}	$W_{tc}, -$	T_{em}	W_{cyl}, W_{fuel}	$T_{ex}, -$
v	p_{dt}	V_{dt}	W_{egr}, W_{out}	T_{dt}	$W_{tc}, -$	$T_{em}, -$

$$F_{out}(t + \delta(t)) = F_{cv}(t) \ , \tag{5}$$

and defining the time delay of the system by $d(t)$, we have

$$F_{out}(t) = F_{cv}(t - d(t)) \tag{6}$$

By comparing (5) and (6), we can obtain the oxygen concentration $F_{cv}(t)$ in the control volume, the oxygen concentration $F_{out}(t)$ at the outlet and the time varying time delay $d(t)$ caused by the transport delay of the system. Moreover, supposing that only the gas mixing occurs in the intake manifold, the oxygen concentration in the intake manifold can be obtained from (1). The relation of the corresponding variables in each subsystem in the considered air path system is shown in Table. 3.

2.2 Mean Value Model of SI Engine

Physical values including pressure, temperature and flow rate at each part are modelled based on the mean value modelling strategy (Guzzella and Onder, 2009; Klasen, 2016).

Modelling of pressure and temperature From the state equation of gas,the first law of thermodynamics and mass conservation law, we have for pressure and temperature at each part from i to v in Fig. 2 that

$$\frac{d}{dt}p_O(t) = \frac{\kappa R}{V_O}[\sum_k W_{I,k}(t)T_{I,k}(t) - T_O(t)\sum_l W_{O,l}] \tag{7}$$

$$\begin{aligned}&\frac{d}{dt}T_O(t)\\ &= \frac{T_O(t)R}{p_O(t)V_O}[\kappa(\sum_k W_{I,k}(t)T_{I,k}(t) - T_O(t)\sum_l W_{O,l}(t))\\ &- (\sum_k W_{I,k}(t) - \sum_l W_{O,l}(t))T_O]\end{aligned} \tag{8}$$

The relation of the corresponding variables in the considered air path system is shown in Table. 4.

Modeling of power Supposing that the power P_c of the compressor has a time constant τ to the power P_t of the turbine, it follows that

$$\dot{P}_c = \frac{1}{\tau}[\eta_m P_t - P_c] \tag{9}$$

with mechanical efficiency of η_m. Moreover, the turbine power is obtained by

Table 5. Correspondence of parameters for mass flow rate

W_I	p_I	A_I	T_I	u_I	p_O
W_{pt}	p_{pt}	A_{pt}	T_{pt}	u_{pt}	p_{im}
W_{wg}	p_{em}	A_{wg}	T_{em}	u_{wg}	p_{dt}
W_{egr}	p_{dt}	A_{egr}	T_{egr}	u_{egr}	p_{uc}
W_{air}	p_{amb}	A_{air}	T_{amb}	-	p_{uc}
W_{out}	p_{dt}	A_{out}	T_{dt}	-	p_{amb}
W_{turb}	p_{em}	A_{turb}	T_{em}	-	p_{dt}

$$P_t = \eta_t c_p \left[1 - \left(\frac{p_{dt}}{p_{em}}\right)^{\frac{\kappa-1}{\kappa}}\right] T_{em} W_{turb} \tag{10}$$

with a turbine efficiency of η_t.

Modelling of mass flow rate The mass flow rate W_I passing through a certain point can be obtained from the equation of the orifice by using the pressure difference as follows:

$$W_I = \frac{A_I p_I}{\sqrt{RT_I}}\psi\left(\frac{p_I}{p_O}\right) \ , \tag{11}$$

where p_I and p_O denote upper and lower pressure, respectively, and A_I is an effective opening area defined by

$$A_I = A_{I,max}\frac{u_I}{100} \tag{12}$$

with a valve opening u_I and maximum effective opening area $A_{I,max}$. The function $\psi(\bullet)$ is simply given by

$$\psi\left(\frac{p_I}{p_O}\right) = \begin{cases} \dfrac{1}{\sqrt{2}} & \left(0 \le \dfrac{p_O}{p_I} < 0.5\right) \\ \sqrt{\dfrac{2p_O}{p_I}\left(1 - \dfrac{p_O}{p_I}\right)} & \left(0.5 \le \dfrac{p_O}{p_I} < 1\right) \end{cases} \tag{13}$$

The relation of the corresponding variables in the considered air path system is shown in Table. 5.

The mass flow rate W_c passing through the compressor is given by

$$W_c = \frac{\eta_c}{c_p T_{uc}\left[\left(\frac{p_{pt}}{p_{uc}}\right)^{\frac{\kappa-1}{\kappa}} - 1\right]} P_c \tag{14}$$

using the compressor power P_c. η_c is a compressor efficiency.

The mass flow rate into the cylinder W_{cyl} is obtained using engine speed N_e, volume efficiency λ as foloows:

$$W_{cyl} = \frac{p_{im}}{RT_{im}}\lambda V_{cyl}\frac{N_e}{120} \tag{15}$$

Supposing that the injection quantity W_{fuel} is given by keeping the theoretical air fuel ratio of 14.7, the injection quantity W_{fuel} is set as

$$W_{fuel} = \frac{1}{14.7}W_{cyl}\frac{F_{im}}{F_{air}} \tag{16}$$

using the oxygen concentration F_{im} in the intake manifold.

Modelling of EGR rate and fresh air flow rate The EGR rate r_{egr} and the fresh air mass flow rate into the cylinder $W_{cyl,air}$ are obtained as follows, respectively.

$$r_{egr} = \left(1 - \frac{F_{im}}{F_{air}}\right) \times 100 \tag{17}$$

and

$$W_{cyl,air} = (1 - r_{egr}/100)W_{cyl} = \frac{F_{im}}{F_{air}} W_{cyl} \tag{18}$$

3. PROBLEM STATEMENT

Consider designing a control system for two-input/two-output engine air path system with the outputs of the fresh air mass $W_{cly,air}$ in the intake manifold and EGR ratio r_{egr}, and the inputs of the throttle valve opening u_{pt} and EGR valve opening u_{egr}.

Although the considered air-path system is nonlinear as modelled in Section 2, we suppose that the transfer function of nominal linear model at a general running point of engine is obtained as follows:

$$G(s) = \begin{bmatrix} G_{11}(s) & G_{12}(s) \\ G_{21}(s) & G_{22}(s) \end{bmatrix}, \tag{19}$$

and it can be modelled by the following decentralized state space model:

$$\begin{aligned} \dot{\boldsymbol{x}}_i(t) &= A_{ii}\boldsymbol{x}_i(t) + \boldsymbol{w}_i(t) + b_i\bar{u}_i(t) \\ y_i(t) &= \boldsymbol{c}_i^T\boldsymbol{x}_i(t) \end{aligned} \tag{20}$$

$$\boldsymbol{w}_i(t) = \sum_{j=1}^{2} B_{ij}\boldsymbol{x}_j(t), \quad B_{ij} = \begin{cases} O & , \ i = j \\ A_{ij} & , \ i \neq j \end{cases} \tag{21}$$
$$i = 1, 2$$

where $i = 1$ represents the intake fresh air system from $u_{pt}(t)$ to $W_{cly,air}(t)$ and $i = 2$ represents the EGR system from $u_{egr}(t - d_2)$ to $r_{egr}(t)$. In the model, we set as

$\bar{u}_1(t) = u_1(t) = u_{pt}(t)$ and $y_1(t) = W_{cly,air}(t)$
$\bar{u}_2(t) = u_2(t - d_2)$, $u_2(t) = u_{egr}(t)$ and $y_2(t) = r_{egr}(t)$

Since there exists a transport delay in the EGR, we modelled the EGR system as a input time delay system, where d_2 is a nominal value of the time delay in the EGR system.

4. OUTPUT PREDICTIVE CONTROL SYSTEM DESIGN

Suppose that the following assumption is satisfied for the each nominal model (20).

Assumption 1. For the system:

$$\begin{aligned} \dot{\boldsymbol{x}}_i(t) &= A_{ii}\boldsymbol{x}_i(t) + b_i\bar{u}_i(t) \\ y_i(t) &= \boldsymbol{c}_i^T\boldsymbol{x}_i(t) \end{aligned} \tag{22}$$

without interference term $\boldsymbol{w}_i(t)$ from the each subsystem given in (20), a parallel feedforward compensator (PFC):

$$\begin{aligned} \dot{\bar{\boldsymbol{x}}}_{fp,i}(t) &= A_{fp,i}\bar{\boldsymbol{x}}_{fp,i}(t) + \boldsymbol{b}_{fp,i}\bar{u}_i(t) \\ \bar{y}_{fp,i}(t) &= \boldsymbol{c}_{fp,i}^T\bar{\boldsymbol{x}}_{fp,i}(t) \ , \end{aligned} \tag{23}$$

which makes the following augmented system having the PFC in parallel with the system (22)

$$\begin{aligned} \dot{\boldsymbol{x}}_{ap,i}(t) &= A_{ap,i}\boldsymbol{x}_{ap,i}(t) + \boldsymbol{b}_{ap,i}\bar{u}_i(t) \\ y_{ap,i}(t) &= \boldsymbol{c}_{ap,i}^T\boldsymbol{x}_{ap,i}(t) \end{aligned} \tag{24}$$

$$\boldsymbol{x}_{ap,i}(t) = \begin{bmatrix} \boldsymbol{x}_i(t) \\ \bar{\boldsymbol{x}}_{fp,i}(t) \end{bmatrix}, \ A_{ap,i} = \begin{bmatrix} A_{ii} & 0 \\ 0 & A_{fp,i} \end{bmatrix}$$
$$\boldsymbol{b}_{ap,i} = \begin{bmatrix} \boldsymbol{b}_i \\ \boldsymbol{b}_{fp,i} \end{bmatrix}, \ \boldsymbol{c}_{ap,i} = \begin{bmatrix} \boldsymbol{c}_i \\ \boldsymbol{c}_{fp,i} \end{bmatrix}$$

have relative degree of 1 and minimum-phase, is known.

Assumption 2. Linear models on some other considered operating points, which may be unknown, can be made minimum-phase and having the relative degree of 1 by the PFC given in Assumption 1.

It should be noted that since $\bar{u}_2(t) = u_2(t - d_2)$, the PFC for the second subsystem (i=2) has delayed input $u_2(t - d_2)$.

Under these assumptions, we propose a robust decentralized output predictive control for fresh-air and EGR system with time delay by modifying the method provided by Mizumoto et al. (2018).

4.1 Output Estimator Design

Consider the augmented subsystems (24) satisfying Assumption 1. The augmented systems have the relative degree of 1 and minimum-phase. Thus, for the augmented system of the considered controlled system (20) with the PFC (23), there exists a nonsingular transformation $\left[y_{ap,i}(t) \ \ \boldsymbol{\eta}_i(t)^T\right]^T = \Phi\boldsymbol{x}_{ap,i}(t)$ such that the augmented system (24) can be transformed into the following canonical form (Isidori, 1995):

$$\begin{aligned} \dot{y}_{ap,i}(t) &= a_{a,i}^* y_{ap,i}(t) + b_{a,i}^*\bar{u}_i(t) + \boldsymbol{c}_{\eta,i}^T\boldsymbol{\eta}_i(t) + \boldsymbol{d}_{w,i}^T\boldsymbol{w}_i(t) \\ \dot{\boldsymbol{\eta}}_i(t) &= A_{\eta,i}\boldsymbol{\eta}_i(t) + \boldsymbol{b}_{\eta,i}y_{ap,i}(t) + F_{w,i}\boldsymbol{w}_i(t) \end{aligned} \tag{25}$$

In (25), $a_{a,i}^*, b_{a,i}^*$ denote practical parameters for an optimal linear model. Unfortunately, since the optimal model for the considered operating point is not known, the system representation given in (25) is not available. Therefore we represent the system by using nominal parameters $a_{a,i}, b_{a,i}$ as follows:

$$\dot{y}_{ap,i}(t) = a_{a,i}y_{ap,i}(t) + b_{a,i}\bar{u}_i(t) + f_i(t) \tag{26}$$

$$\begin{aligned} f_i(t) =& \Delta a_{a,i}y_{ap,i}(t) + \Delta b_{a,i}\bar{u}_i(t) \\ &+ \boldsymbol{c}_{\eta,i}^T\boldsymbol{\eta}_i(t) + \boldsymbol{d}_{w,i}^T\boldsymbol{w}_i(t) \end{aligned} \tag{27}$$

with $\Delta a_{a,i} = a_{a,i}^* - a_{a,i}$, $\Delta b_{a,i} = b_{a,i}^* - b_{a,i}$. $f_i(t)$ indicates uncertainty of the system caused by model mismatch. It may include uncertain nonlinear properties. Thus the system can be modelled as an output equation form as in (27) with uncertain function $f_i(t)$.

Now, design the output estimator for the system (26) as

$$\begin{aligned} \dot{z}_{1,i}(t) =& a_{a,i}z_{1,i}(t) + b_{a,i}\bar{u}_i(t) + z_{1,i}(t) \\ &+ k_{1,i}(y_{ap,i}(t) - z_{1,i}(t)) \end{aligned} \tag{28}$$

$$\dot{z}_{2,i}(t) = k_{2,i}(y_{ap,i}(t) - z_{1,i}(t)), \tag{29}$$

where $z_{1,i}(t)$ is the estimated value of $y_{ap,i}(t)$ and $z_{2,i}(t)$ is the estimated value of $f_i(t)$. the design parameters $k_{1,i}$ and $k_{2,i}$ are set such that

$$A_{0,i} = \begin{bmatrix} a_{a,i} - k_{1,i} & 1 \\ -k_{2,i} & 0 \end{bmatrix} \tag{30}$$

is a stable matrix.

4.2 Output Predictor

Based on the form of designed output estimator (28), we consider the following output predictor from a current time t_0 for the augmented system:

$$\begin{aligned}\dot{\hat{\bar{y}}}_{ap,i}(t) &= a_{a,i}\hat{\bar{y}}_{ap,i}(t) + b_{a,i}\bar{v}_i(t) + z_{2,i}(t_0) \\ \hat{\bar{y}}_{ap,i}(t_0) &= z_{1,i}(t_0) \quad , \quad t \geq t_0\end{aligned} \tag{31}$$

with a predictive control input $\bar{v}_i(t)$ that is to be determined later.

In the designed output predictor, $z_{2,i}(t_0)$ is a compensation term for uncertain function $f_i(t)$ so that one can design a robust output predictor with respect to model mismatch on the given nominal model.

It should also be noted that the designed output predictor is the one for the augmented system with the given PFC (23).

Therefore, the predicted virtual ideal output for the practical system is obtained from the structure of the augmented system (24) by

$$\begin{aligned}\hat{\bar{y}}_i(t) &= \hat{\bar{y}}_{ap,i}(t) - y_{fp,i}(t) \\ &= \hat{\bar{y}}_{ap,i}(t) - c_{fp,i}^T \boldsymbol{x}_{fp,i}(t) \\ &= \bar{c}_{ap,i}^T \bar{\boldsymbol{x}}_{ap,i}(t) \ ,\end{aligned} \tag{32}$$

with

$$\bar{\boldsymbol{x}}_{ap,i}(t) = \begin{bmatrix} \hat{\bar{y}}_{ap,i}(t) \\ \boldsymbol{x}_{fp,i}(t) \end{bmatrix} \ , \ \ \bar{c}_{ap,i}^T = \begin{bmatrix} 1 \ , & -c_{fp,i}^T \end{bmatrix}$$

where $\boldsymbol{x}_{fp,i}(t)$ and $y_{fp,i}(t)$ are the state and output of the PFC (23) with the input of $u_i(t)$ without time delay.

$$\begin{aligned}\dot{\boldsymbol{x}}_{fp,i}(t) &= A_{fp,i}\boldsymbol{x}_{fp,i}(t) + b_{fp,i}u_i(t) \\ y_{fp,i}(t) &= \boldsymbol{c}_{fp,i}^T \boldsymbol{x}_{fp,i}(t)\end{aligned} \tag{33}$$

The state equation of the defined $\bar{\boldsymbol{x}}_{ap,i}$-system can be expressed by

$$\dot{\bar{\boldsymbol{x}}}_{ap,i}(t) = \bar{A}_{ap,i}\bar{\boldsymbol{x}}_{ap,i}(t) + \bar{B}_{ap,i}\bar{\boldsymbol{v}}_{ap,i}(t) \tag{34}$$

with

$$\bar{A}_{ap,i} = \begin{bmatrix} a_{a,i} & O \\ O & A_{fp,i} \end{bmatrix} \ , \ \bar{B}_{ap,i} = \begin{bmatrix} b_{a,i} & 1 \\ b_{fp,i} & 0 \end{bmatrix}$$
$$\bar{\boldsymbol{v}}_{ap,i}(t) = \begin{bmatrix} \bar{v}_i(t) \\ z_{2,i}(t_0) \end{bmatrix}$$

Using this output predictor we consider designing an output predictive controller based on the method provided in Mizumoto et al. (2018).

Remark 1. The reason why the PFC stats with the input having no time delay is used in the output predictor is that we consider designing optimal current input in the following predictive control.

4.3 Output Predictive Controller Design

We consider to find a control input $\bar{v}(t)$ minimizing the following cost function J_i:

$$\begin{aligned}J_i = &\frac{1}{2}\bar{\boldsymbol{x}}_{ap,i}^T(t_f)P_{f,i}\bar{\boldsymbol{x}}_{ap,i}(t_f) \\ &+ \int_{t_0}^{t_f} \frac{1}{2}\left\{\hat{\bar{e}}_i(t)^2 + r_i\bar{v}_i(t)^2\right\} dt\end{aligned} \tag{35}$$
$$\hat{\bar{e}}_i(t) = \hat{\bar{y}}_i(t) - y_{m,i}(t)$$

under the equality constrain in (34) and the following terminal constrain:

$$\begin{aligned}\hat{\bar{e}}_i(t_f) &= \hat{\bar{y}}_i(t_f) - y_{m,i}(t_f) \\ &= \bar{c}_{ap,i}^T \bar{\boldsymbol{x}}_{ap,i}(t_f) - y_{m,i}(t_f) = 0,\end{aligned} \tag{36}$$

where $P_{f,i} = P_{f,i} > 0$ and $r_i > 0$ are weights.

It is well recognized that the optimization problem of (35) can be solved as the following Euler-Lagrange equation by introducing Lagrange multipliers $\boldsymbol{\lambda}_i$, $\nu_{f,i}$:

$$\dot{\bar{\boldsymbol{x}}}_{ap,i}(t) = \bar{A}_{ap,i}\bar{\boldsymbol{x}}_{ap,i}(t) + \bar{B}_{ap,i}\bar{\boldsymbol{v}}_i(t) \tag{37}$$

$$\bar{\boldsymbol{x}}_{ap,i}(t_0) = \begin{bmatrix} \hat{y}_{ap,i}(t_0) \\ \bar{\boldsymbol{x}}_{fp,i}(t_0) \end{bmatrix} \tag{38}$$

$$\dot{\boldsymbol{\lambda}}_i(t) = -\bar{\boldsymbol{c}}_{ap,i}\hat{\bar{e}}_i(t) - \bar{A}_{ap,i}^T\boldsymbol{\lambda}_i(t) \tag{39}$$

$$\bar{v}_i(t) = -\frac{1}{r_i}\bar{\boldsymbol{b}}_{ap,i}^T\boldsymbol{\lambda}_i(t) \tag{40}$$

$$\boldsymbol{\lambda}_i(t_f) = P_{f,i}\bar{\boldsymbol{x}}_{ap,i}(t_f) + \nu_{f,i}\bar{\boldsymbol{c}}_{ap,i} \tag{41}$$

$$\bar{\boldsymbol{b}}_{ap,i} = \begin{bmatrix} b_{a,i} \\ \boldsymbol{b}_{fp,i} \end{bmatrix}$$

From this results, the optimal predictive input $\bar{v}(t)$ is obtained from (40) by solving (39) with the initial condition $\boldsymbol{\lambda}_i(t_0)$ which leads to satisfy (41) with a $\nu_{f,i}$.

The initial condition $\boldsymbol{\lambda}_i(t_0)$ and a value of $\nu_{f,i}$ that ensures the relation in (41) are obtained as follows from the given and known conditions as follows (Mizumoto et al., 2018):

$$\begin{aligned}\begin{bmatrix} \boldsymbol{\lambda}_i(t_0) \\ \nu_{f,i} \end{bmatrix} = &\begin{bmatrix} M_{4,i}(t_f) - P_{f,i}M_{2,i}(t_f) & -\bar{\boldsymbol{c}}_{ap,i} \\ \bar{\boldsymbol{c}}_{ap,i}^T M_{2,i}(t_f) & 0 \end{bmatrix}^{-1} \\ &\times \begin{bmatrix} P_{f,i}W_{1,i}(t_f) - W_{2,i}(t_f) \\ y_{m,i}(t_f) - \bar{\boldsymbol{c}}_{ap,i}^T W_{1,i}(t_f) \end{bmatrix}\end{aligned} \tag{42}$$

with

$$\begin{aligned}M_i(t_f) &= \begin{bmatrix} M_{1,i}(t_f) & M_{2,i}(t_f) \\ M_{3,i}(t_f) & M_{4,i}(t_f) \end{bmatrix} = e^{A_i^*(t_f - t_0)} \\ W_{1,i}(t_f) &= M_{1,i}(t_f)\bar{\boldsymbol{x}}_{ap,i}(t_0) + \boldsymbol{a}_{1,i}(t_f) \\ W_{2,i}(t_f) &= M_{3,i}(t_f)\bar{\boldsymbol{x}}_{ap,i}(t_0) + \boldsymbol{a}_{2,i}(t_f),\end{aligned}$$

where

$$\begin{aligned}A_i^* &= \begin{bmatrix} \bar{A}_{ap,i} & -\frac{1}{r_i}\bar{\boldsymbol{b}}_{ap,i}\bar{\boldsymbol{b}}_{ap,i}^T \\ -\bar{\boldsymbol{c}}_{ap,i}\bar{\boldsymbol{c}}_{ap,i}^T & -\bar{A}_{ap,i}^T \end{bmatrix} \\ \begin{bmatrix} \boldsymbol{a}_{1,i}(t_f) \\ \boldsymbol{a}_{2,i}(t_f) \end{bmatrix} &= \int_0^{t_f - t_0} e^{A_i^*\tau} \begin{bmatrix} \boldsymbol{0} & 1 \\ \bar{\boldsymbol{c}}_{ap,i}\boldsymbol{0} \end{bmatrix} \begin{bmatrix} y_{m,i}(t_f - \tau) \\ z_{2,i}(t_0) \end{bmatrix} d\tau\end{aligned} \tag{43}$$

The obtained predictive control input $\bar{v}_i(t)$ is the optimal input, and thus we design the practical optimal control input $u_i(t)$ by

$$u_i(t) = \bar{v}_i(t) \tag{44}$$

for a given interval $t \in [t_0, t_1)$ $(t_1 \leq t_f)$

5. VALIDATION THROUGH NUMERICAL SIMULATION

The effectiveness of the proposed method is validated through numerical simulations for an air path system given in the section 2.

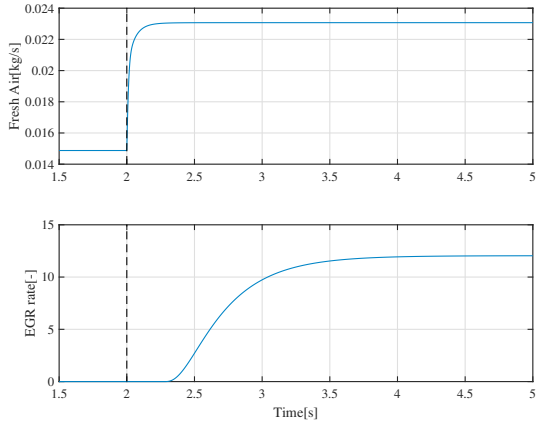

Fig. 4. Step response for identification

5.1 Control System Design

In order to design the proposed decentralized output predictive control system, we first obtain simple nominal models from the throttle valve opening u_{pt} to the fresh air mass $W_{cly,air}$ and from the EGR valve opening u_{egr} to EGR ratio r_{egr} using the information about step responses shown in Fig. 4.

The obtained linear model from u_{pt} to $W_{cly,air}$ and from u_{egr} to r_{egr} are given by

$$
\begin{aligned}
G_{nom,11}(s) &= \bar{G}_{nom,11}(s) \\
\bar{G}_{nom,11}(s) &= \frac{2.215e05s^7 + 1.029e08s^6 + 2.88e10s^5}{s^{10} + 1916s^9 + 1.617e06s^8 + 7.773e08s^7} \\
&\quad \frac{+4.789e12s^4 + 4.26e14s^3}{+2.301e11s^6 + 4.229e13s^5 + 4.637e15s^4} \\
&\quad \frac{+1.488e16s^2 + 2.07e17s + 9.57e17}{+2.74e17s^3 + 7.32e18s^2 + 8.53e19s + 3.50e20} \\
G_{nom,22} &= \bar{G}_{nom,22}(s)e^{-0.3s} \\
\bar{G}_{nom,22}(s) &= \frac{6.273e07s^2 + 1.968e09s}{s^5 + 2814s^4 + 8.259e07s^3 + 2.939e09s^2} \\
&\quad \frac{+2.955e10}{+2.573e10s + 5.498e10}
\end{aligned} \tag{45}
$$

The PFC for output estimation and prediction is designed as

$$H_{est,i} = G_{est,i} - \bar{G}_{nom,ii} \tag{46}$$

by considering ideal augmented systems $G_{est,i}$ given by

$$G_{est,1} = \frac{10^{-3}}{s + 10^{-6}},\ G_{est,2} = \frac{10^{-3}}{s + 10^{-5}} \tag{47}$$

The design parameters in the controller are set as

$$
\begin{aligned}
&k_{1,1} = 5 \times 10^2\ , k_{2,2} = 1 \times 10^2 \\
&r_1 = 10^{-2}\ , P_{f,1} = 10^{-2} I \\
&k_{1,2} = 5, k_{2,2} = 0.3 \\
&r_2 = 10^{-4}\ , P_{f,2} = 10^{-4} I\ , t_f = 5[\text{ms}]
\end{aligned}
$$

$a_{a,i}, b_{a,i}$ in the output estimator are set from (47) by

$$
\begin{aligned}
a_{a,1} &= -10^{-2}\ , b_{a,1} = 10^{-5} \\
a_{a,2} &= -10^{-4}\ , b_{a,2} = 10^{-4}
\end{aligned}
$$

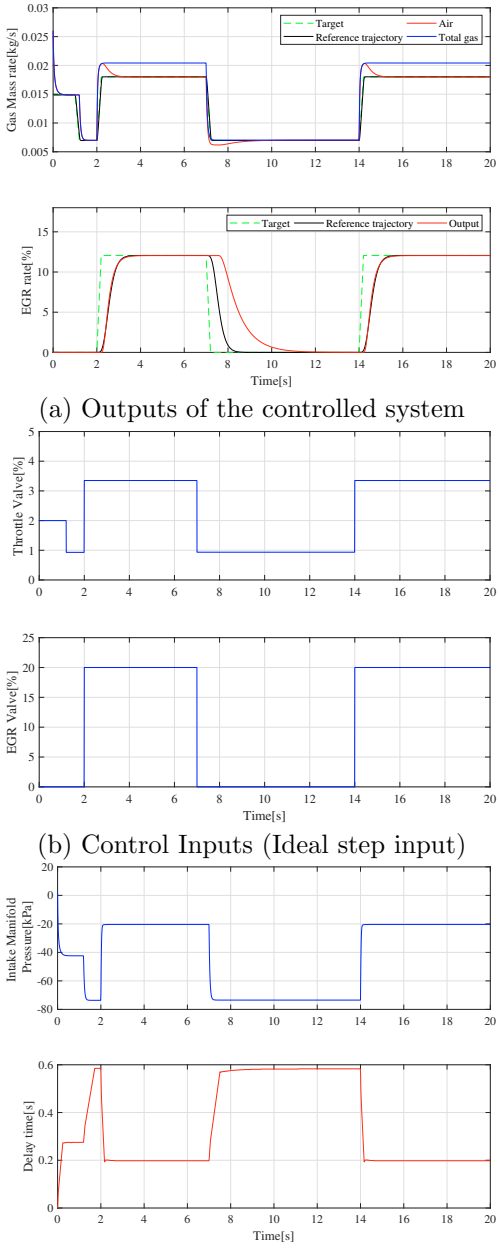

(a) Outputs of the controlled system

(b) Control Inputs (Ideal step input)

(c) Intake manifold pressure and transport delay of EGR

Fig. 5. Simulation results without control

5.2 Simulation Results

In order to recall the problem again, we did simulation by ideal step inputs. The result is shown in Fig. 5. As shown in Fig. 5(a), the overshoot/undershoot phenomena for the fresh air mass flow rate were caused by the transport delay of EGR. The delay, which is varying according to the situation, is shown in Fig. 5(c). The overshoot/undershoot phenomena on the fresh air mass flow rate affect fuel consumption and causes a torque overshoot and/or deterioration of the ride quality in the automobiles.

Fig. 6 shows the results with the proposed method in which the output estimator was designed based on the nominal model given in (45) with a time delay of 0.3[s].

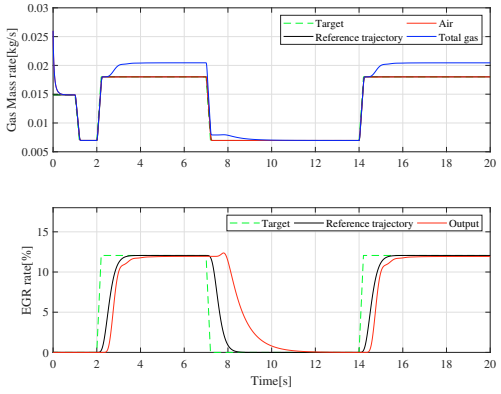

(a) Outputs of controlled system

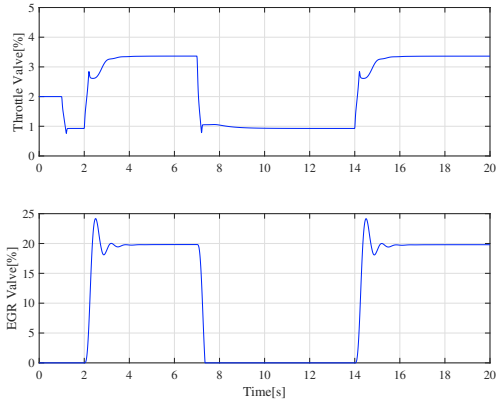

(b) Control input

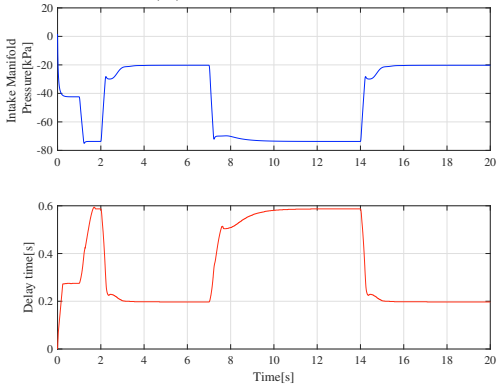

(c) Intake manifold pressure and transport delay of EGR

Fig. 6. Simulation results of nominal delay 0.3[s]

Even though the considered air path system has a time-varying time delay, the propose method can handle the delay well and good control performance without over-shoot/undershoot phenomena on the fresh air mass rate is obtained.

In addition to the above simulation, we confirm the effectiveness of the proposed method through a simulation according to a driving scenario shown in Fig. 7 in order to validate the control performance in the transient state. In the simulation, we used the same design parameters as given in the previous simulation except the nominal value of time-delay, and the output estimator was designed based on the nominal model given in (45) with a time delay of 0.25[s].

Fig. 8 shows the results with the proposed method. Although the controller was designed based on a nominal

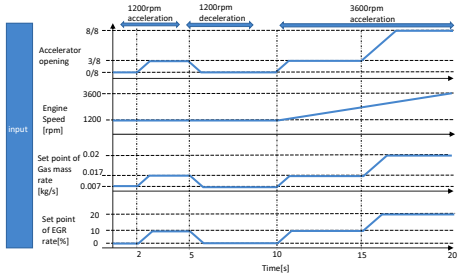

Fig. 7. Driving scenario

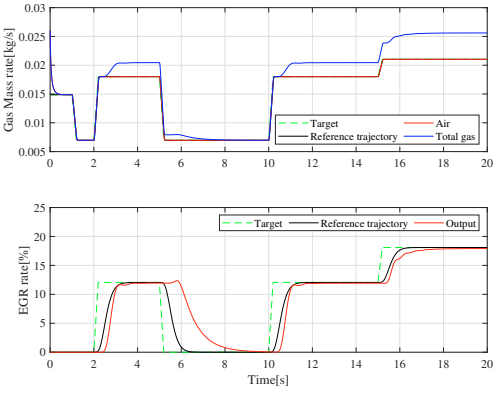

(a) Outputs of controlled system

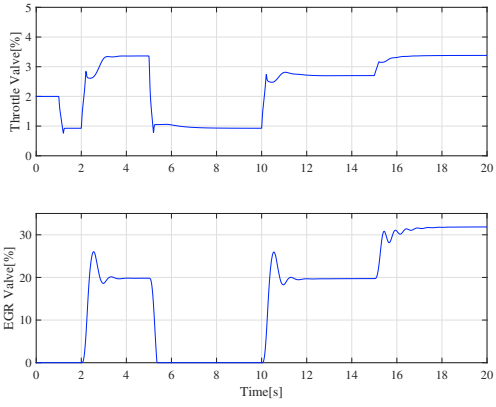

(b) Control input

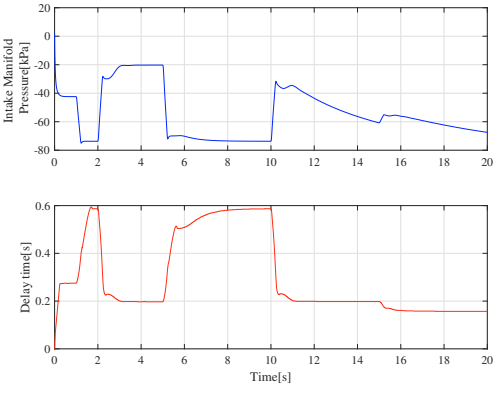

(c) Intake manifold pressure and transport delay of EGR

Fig. 8. Simulation results according to the driving scenario in Fig. 7

model, the control performance with the proposed method was maintained even for the case in transient state in which the accelerator was pressed harder on.

6. CONCLUSION

In this paper, a modeling and control of an engine air path system was considered. The detailed mean value model of air path system with time delay due to EGR transfer delay was derived based on a physics-based time-varying transport delay modeling, and a decentralized output predictive control was proposed to deal with the considered MIMO air path system. In the considered air path system, there exists a time delay due to the transport delay of the EGR. A robust output estimator with a PFC for time delay system was also proposed by taking the nominal delay into consideration. The effectiveness of the proposed method was confirmed through numerical simulations for the derived air path model with time-varying time delay.

ACKNOWLEDGEMENTS

This work is the result of a collaborative research program with the Research association of Automotive Internal Combustion Engines (AICE) for fiscal year 2020. The authors gratefully acknowledge the concerned personnel.

REFERENCES

Ferreau, H.J., Ortner, P., Langthaler, P., del Re, L., and Diehl, M. (2007). Predictive control of a real-world diesel engine using an extended online active set strategy. *Annual Reviews in Control*, 31, 293–301.

Gelso, E.R. and Lindberg, J. (2014). Air-path model predictive control of a heavy-duty diesel engine with variable valve actuation. *Proc. of the 19th World Congress IFAC, Cape Town, South Africa. August 24-29*, 3012–3017.

Guzzella, L. and Onder, C. (2009). Introduction to modeling and control of internal combustion engine systems. *Springer*.

Herceg, M., Raff, T., Findeisen, R., and Allg ower, F. (2006). Nonlinear model predictive control of a turbocharged diesel engine. *Proc. of the IEEE CCA 2006*, 2766–2771.

Isidori, A. (1995). *Nonlinear Control Systems*. Springer, 3rd edition.

Kekik, B. and Akar, M. (2019). Model predictive control of diesel engine air path with actuator delays. *IFAC PapersOnLine*, 52(18), 150–155.

Klasen, E. (2016). Modeling and estimation of long route egr mass flow in turbocharged gasoline engine. *Master Thesis, Linkoping University in Electrical Engineering*.

Mizumoto, I. and Fujii, S. (2017). Aspr based output feedback control with an adaptive predictive feedfoward input for mimo systems. *Proceedings of 20th IFAC World Congress, Toulouse, France, July 9-14*, 5480–5485.

Mizumoto, I., Fujimoto, Y., and Ikejiri, M. (2015). Adaptive output predictor based adaptive predictive control with aspr constraint. *Automatica*, 57, 152–163.

Mizumoto, I., Murakami, S., and Masuda, S. (2018). Aspr based adaptive output feedback control with an output predictive feedforward input for continuous-time systems. *Proc. of the 57th IEEE Conference on Decision and Control*, 613–619.

Nielsen, K.V., Blanke, M., Eriksson, L., and M.V.-Laursen (2017). Adaptive feedforward control of exhaust recirculation in large diesel. *Control Engineering Practice*, 65, 26–35.

Ortner, P., Bergmann, R., Ferreau, H.J., and del Re, L. (2009). Nonlinear model predictive control of a diesel engine airpath. *IFAC Proceedings Volumes*, 42(2), 91–96.

Zeng, X. and Wang, J. (2014). A physics-based time-varying transport delay oxygen concentration model for dual-loop exhaust gas recirculation (egr) engine airpaths. *Applied Energy*, 125, 300–307.